

# Optical and structural parameters of the ZnO thin film grown by pulsed filtered cathodic vacuum arc deposition

Ebru Şenadım, Sıtkı Eker, Hamide Kavak\*, Ramazan Esen

*Physics Department, Cukurova University, 01330, Adana, Turkey*

Received 31 May 2006; received in revised form 19 June 2006; accepted 1 July 2006 by H. Akai

Available online 18 July 2006

## Abstract

Transparent conductive ZnO film was deposited on glass substrate by pulsed filtered cathodic vacuum arc deposition (PFCVAD). Optical parameters such as absorption coefficient  $\alpha$ , the refractive index  $n$ , energy band gap  $E_g$  and dielectric constants have been determined using different methods. Kramers–Kronig and dispersion relations were employed to determine the complex refractive index and dielectric constants using reflection data in the ultraviolet–visible–near infrared regions. The spectra of the dielectric coefficient were used to calculate the energy band gap and the value was 3.24 eV. The experimental energy band gap was found to be 3.22 eV for 357 nm thick ZnO thin film. The envelope method was also used to calculate the refractive index and the data were consistent with K–K relation results. The structure of the film was analyzed with an x-ray diffractometer and the film was polycrystalline in nature with preferred (002) orientation.

© 2006 Elsevier Ltd. All rights reserved.

PACS: 78.20-e; 78.20.Ci; 78.20.Bh; 81.05.Dz; 81.15.Ef

Keywords: A. ZnO thin film; B. Pulsed filtered cathodic vacuum arc deposition; B. Structural properties; D. Optical properties

## 1. Introduction

Transparent conducting oxide (TCO) films have found extensive applications in optoelectronic devices [1] (for example, solar cells [2], liquid crystal displays, heat mirrors and multiplayer photothermal conversion systems [3]). Zinc oxide has attracted attention as a transparent conducting oxide because of its (i) large band gap (3.3 eV) [4], (ii) high conductivity, (iii) ease in doping, (iv) chemical stability in hydrogen plasma [5], (v) thermal stability when doped with III group elements [6], and (vi) abundance in nature and nontoxicity. In addition to potential use as transparent conducting oxide in optoelectronic devices, ZnO thin films also find application as gas sensors [6], because of their high electrical resistivity.

Several deposition techniques are used to grow zinc oxide (ZnO) thin films. These include chemical vapor deposition

(CVD) [7,8], magnetron sputtering [9–12], cathodic vacuum arc deposition (CVAD), spray pyrolysis [13,14], and pulsed laser deposition (PLD) [15,16]. The filtered cathodic vacuum arc, another energetic deposition technique, has recently received little attention for the preparation of ZnO films. Naoe and Nakagawa prepared ZnO films at temperature 600 °C by a vacuum arc without macroparticle filtering [17]. Takikawa et al. deposited *c*-axis oriented ZnO films by a simple shielded vacuum arc without external heating in the pressure range of  $1 \times 10^{-3}$ – $4 \times 10^{-2}$  Torr, where the distance between the cathode and substrate was 20 cm [18].

In comparison with other techniques, pulsed filtered cathodic vacuum arc deposition (PFCVAD) provide high density, high adhesion, excellent coating uniformity of thin films at low deposition temperatures [19]. Besides these advantages nearly 100% ionization of the cathode materials in the plasma means that the impact energy of the depositing ions at the growth surface can be readily controlled using electric fields. Their high-energy plasma plume will readily ionize most background gases. These features make the pulsed cathodic vacuum arc an ideal source for the production of metal oxides and nitrides [19]. And also the PFCVAD technique provides

\* Corresponding address: Cukurova University, Science and Art Faculty, Physics Department, TR01330/Adana, Turkey. Tel.: +90 322 3386801; fax: +90 322 3386070.

E-mail address: [hkavak@cu.edu.tr](mailto:hkavak@cu.edu.tr) (H. Kavak).

thickness control at the atomic scale and there is no need to cool the system.

The envelope method has been developed for transmittance measurements to evaluate the refractive index, extinction coefficient and absorption coefficient [15]. In the optical transmission spectrum multiple coherent reflections are present due to interference effect and the above parameters can be determined from the envelopes,  $T_{\max}$  and  $T_{\min}$  along the interference maxima and minima.

The Kramers–Kronig [K–K] relations have been widely used in the analysis of reflection spectra, and much of the discussion in the literature about this method has been concerned with the adequacy of various methods proposed for the evaluation of the integrals which in principle run from  $0 < \lambda < \infty$ .

This paper reports the growth of ZnO film on glass substrate by the pulsed filtered cathodic vacuum arc deposition method. Structural and optical properties of PFCVAD ZnO thin film such as x-ray diffraction, transmittance, refractive index and energy band gap are studied. The envelope method was employed to determine refractive index and extinction coefficient as a function of wavelength. Kramers–Kronig and dispersion relations were also used to evaluate refractive index, complex dielectric constant and dispersion energy using reflection spectra.

## 2. Experimental and computational methods

### 2.1. Sample preparation and characterization

The details of the PFCVAD system have been described elsewhere. The cylindrical vacuum chamber was made of stainless steel (486 mm diameter and 385 mm in length) and evacuated using a primary and a turbomolecular pump (500 l/s) to a base pressure below  $1.3 \times 10^{-8}$  Torr [20].

In this system, metallic zinc (1 mm in diameter and purity 99.99%) which was held in an alumina ceramic tube was employed as an cathode target, and oxygen (purity 99.9999%) was employed as the reactive gas. Film was deposited on ultrasonically cleaned glass substrate which was located 14 mm away from the anode. Oxygen gas was input into the chamber directly by a mass flow controller with constant flow rate of 135 sccm. In this study deposition parameters for ZnO thin film were as follows: oxygen gas flow rate 135 sccm, oxygen pressure during the deposition  $5 \times 10^{-4}$  Torr, in fixed arc current of 650 A, substrate temperature 25 °C. The distance from the target to the substrate was maintained to be 14 mm.

The x-ray diffraction technique was used to specify the structural parameters, the existent phases and the orientation of as-deposited ZnO thin film. The x-ray diffraction measurements was performed by using a Rigaku Miniflex x-ray diffraction system equipped with Cu K- $\alpha$  radiation of average wavelength 1.54059 Å. X-ray diffractograms were taken for  $2\theta$  in between 20° and 70° and scan speed of 2 degree/min.

The optical properties of ZnO thin film deposited by PFCVAD were carried out by a double beam computer controlled spectrophotometer (Perkin Elmer Lambda 2S) in

the UV/VIS/NIR regions. The optical transmittance and reflection at normal incidence were recorded in the wavelength range of 190–1100 nm. Swanepoel's envelope method and the Kramers–Kronig relation were employed to evaluate the refractive index,  $n$ , as a function of wavelength. The thickness of ZnO thin film was determined from interference fringes of transmission data measured over the visible range. And also a Filmetrics model F30 was employed to measure the thickness of the ZnO thin film. The F30 is a spectral reflectance system that measures the thickness and optical constants of translucent thin film layers on opaque and transparent substrates.

### 2.2. Calculation of refractive index using the envelope method

Envelope method is commonly used to determine optical constants such as refractive index  $n$ . The widely used version of the envelope method has been developed by Swanepoel [21] for transmittance measurement. Versions based on the reflectance alone are infrequent [22–24], the extraction of the optical constants is more involved and very different. For the method proposed by Swanepoel, the optical constants are deduced from the fringe patterns in the transmittance spectrum. In the transmittance region where the absorption coefficient  $\alpha = 0$ , the refractive index  $n$  is given by [25]:

$$n = [N + (N^2 - n_s^2)^{1/2}]^{1/2} \quad (1)$$

where

$$N = \frac{2n_s}{T_{\min}} - \frac{(n_s^2 + 1)}{2} \quad (2)$$

$T_{\min}$  is the envelope function of the transmittance minima and  $n_s$  is the refractive index of the substrate.

In the region of weak and medium absorption, where  $\alpha \neq 0$ , the transmittance decreases mainly due to the effect of absorption coefficient  $\alpha$  and the refractive index  $n$  is given by:

$$n = [N + (N^2 - n_s^2)^{1/2}]^{1/2} \quad (3)$$

where

$$N = \frac{(n_s^2 + 1)}{2} + 2n_s \frac{(T_{\max} - T_{\min})}{T_{\max} T_{\min}} \quad (4)$$

and  $T_{\max}$  is the envelope function of the transmittance maximum.

### 2.3. Kramers–Kronig and dispersion analysis

Kramers–Kronig transformation has been used extensively to determine the complex refractive index  $\hat{n} = n + ik$  ( $n$  refractive index,  $k$  extinction coefficient) and the complex dielectric function  $\hat{\epsilon} = \epsilon_1 + i\epsilon_2$  ( $\epsilon_1$  real and imaginary  $\epsilon_2$  part of dielectric function) from the reflection spectra [26–28]. The measured reflectance spectrum of an optically thick sample consists of two components. One component is the actual absorbance spectrum, and the other is the refractive index spectrum. The K–K transformation will decompose the complex reflectance spectrum into its separate extinction

coefficient and refractive index spectra. This information can be used for qualitative evaluation of the sample. The extinction coefficient spectrum can be used to produce the absorbance spectrum [29].

In the simplest and most widely used application, the reflectivity is measured at normal incidence from air ambience. The phase shift  $\theta(\lambda)$  can be calculated in terms of the Fresnel reflection coefficient

$$\theta(\lambda_0) = \frac{2\lambda_0}{\pi} \left[ \int_0^\infty \frac{\ln \sqrt{R(\lambda)} d\lambda}{\lambda^2 - \lambda_0^2} \right]. \quad (5)$$

The real and imaginary components of the complex refractive index can be calculated from the experimental reflectance spectrum using K–K transformations as the following formula:

$$n(\lambda) = \frac{1 - R(\lambda)}{1 + R(\lambda) - 2\sqrt{R(\lambda)} \cos(\theta(\lambda))} \quad (6)$$

$$k(\lambda) = \frac{-2\sqrt{R(\lambda)} \sin(\theta(\lambda))}{1 + R(\lambda) - 2\sqrt{R(\lambda)} \cos(\theta(\lambda))} \quad (7)$$

where  $R$  is the reflectance spectrum,  $\lambda$  is the wavelength and  $\theta$  is the phase shift angle of the sample. The refractive index and extinction coefficient can be determined as a function of wavelength by substituting reflectance data and phase shift  $\theta(\lambda)$  Eq. (5) into Eqs. (6) and (7).

The real and imaginary parts of complex dielectric index can be calculated from the following formula:

$$\begin{aligned} \epsilon_1(\lambda) &= n^2(\lambda) - k^2(\lambda) \\ \epsilon_2(\lambda) &= 2n(\lambda)k(\lambda) \end{aligned} \quad (8)$$

The values of the dispersive refractive index were analyzed using the single oscillator model developed by Wemple et al. [30]. According to dispersion theory, generally in the region of low absorption the index of refraction  $n$  of a dielectric media is given by,

$$n^2(E) = 1 + \frac{E_{\text{osc}} E_d}{E_{\text{osc}}^2 - E^2} \quad (9)$$

where  $E_d$  is the dispersion energy and  $E_{\text{osc}}$  the single effective oscillator energy and  $E$  the photon energy.  $E_d$  is a parameter that weighs the strength of interband optical transitions. Plotting  $(n^2 - 1)^{-1}$  versus  $E^2$  allows the determination of the oscillator parameters, by fitting a straight line to the data at the higher wavelength (lower energy) region.

### 3. Results and discussion

#### 3.1. Structural properties of PFCVAD ZnO film

The crystalline quality and orientation of the as-deposited ZnO thin film has been investigated by x-ray diffraction (XRD). A typical XRD spectrum of a sample deposited with oxygen pressure of  $5 \times 10^{-4}$  Torr is presented in Fig. 1. This film has polycrystalline hexagonal wurtzite structure with dominant  $c$ -axis orientation.

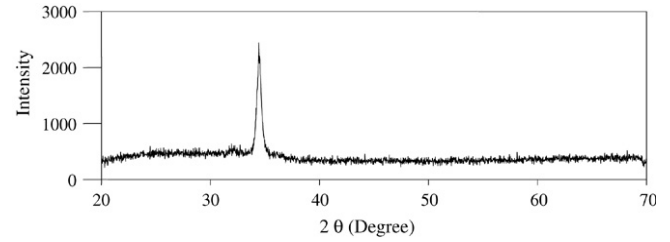


Fig. 1. XRD pattern of ZnO thin film prepared on glass substrate.

The peak position and intensity of ZnO thin film with (002) orientation is located at  $2\theta = 34.44^\circ$ , 2443.33 a.u., respectively. The value of FWHM for the (002) diffraction peak of ZnO deposited on glass substrate is  $0.369^\circ$ . To evaluate the mean grain size  $D$  of ZnO on the basis of the XRD results, the Scherrer formula

$$D = \frac{0.9\lambda}{\beta \cos \theta}$$

was applied, where  $\lambda$ ,  $\beta$ ,  $\theta$  are x-ray wavelength (1.54056 Å), the FWHM of the ZnO (002) diffraction peak and the Bragg diffraction angle, respectively. By this calculation, the mean grain size of the ZnO deposited on glass substrate is found 22.5 nm.

The crystal lattice constant  $c$  could be obtained by the Bragg equation. From the wavelength of the x-rays and the diffraction angle all peaks in the diffraction pattern was identified using equation  $n\lambda = 2d \sin \theta$ , where  $n$  is the order of the diffracted beam,  $\lambda$  is the wavelength of the x-rays,  $d$  is the inter-planar distance of the diffracting planes and  $\theta$  is the angle between the incoming x-rays and the normal of the diffracting planes. The value of inter-planar distance  $d$  for  $5 \times 10^{-4}$  Torr was 0.260 nm. XRD measurement shows that the sample is wurtzite (hexagonal) structured ZnO thin film with lattice constants of 0.520 nm.

#### 3.2. Optical properties of PFCVAD ZnO film

The optical transmittance spectrum of PFCVAD as-deposited ZnO film was recorded at room temperature using a double beam spectrometer. The thickness of the zinc oxide thin film was evaluated from the interference fringes. The thickness was found to be 357 nm and this value is verified with a Filmetrics instrument. The optical transmittance and reflectance spectra of a 357 nm thick ZnO film deposited on glass substrate are shown in Fig. 2. The maximum of transmittance of the film is about 95%.

The absorption coefficient values were used to evaluate the optical energy band gap of ZnO thin film employing optical absorption spectra. The relation between absorption coefficient and the incident photon energy is given by [31]

$$\alpha h\nu = B (h\nu - E_g)^n \quad (10)$$

where  $B$  is constant and  $E_g$  is the optical energy gap. For a direct transition a value of  $n = \frac{1}{2}$  was found to be most suitable for ZnO thin film. The optical energy band gap and

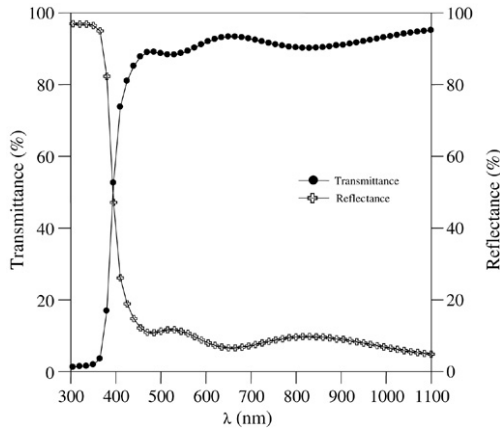


Fig. 2. Transmittance and reflectance spectra for the ZnO thin film grown on glass substrate.

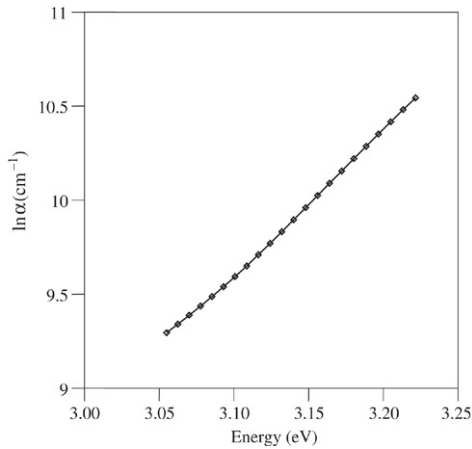


Fig. 3. Semi-logarithmic plots of absorption coefficient as a function of energy for the ZnO thin film.

the absorption edge of ZnO thin film are 3.22 eV and 386 nm, respectively.

The band tailing (Urbach energy) is the effect of impurity or disorder and any other defects. In the exponential-edge region, the absorption coefficient is expressed by the so-called Urbach relationship [32]

$$\alpha(h\nu) = AE_0^{3/2} \exp(h\nu/E_0) \quad \text{for } h\nu < E_g \quad (11)$$

where,  $A$  is a constant and  $E_0$  (Urbach energy) is a parameter describing the width of the localized state in the band gap due to the above mentioned effects, which characterizes the slope of the exponential edge region. We plotted the curve of  $\ln(\alpha)$  vs photon energy, as shown in Fig. 3 and the  $E_0$  value was calculated from the slope of this curve and was found as 0.130 eV for PFCVAD ZnO thin film.  $E_0$  characterizes the slope of the exponential-edge region and the inverse of the slope gives width of the localized states associated with the amorphous state in the band gap of the thin film. The Urbach's absorption edge is formed in the region of photon energies below the forbidden band gap. The interaction between lattice vibrations and localized states in the tail of the band gap of the

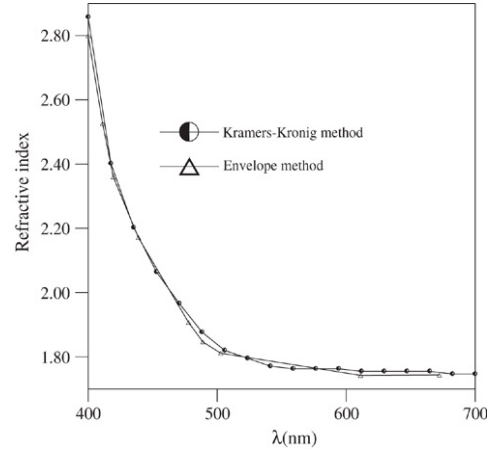


Fig. 4. Wavelength dependence of refractive index  $n(\lambda)$  for the ZnO films using KK relation and envelope method.

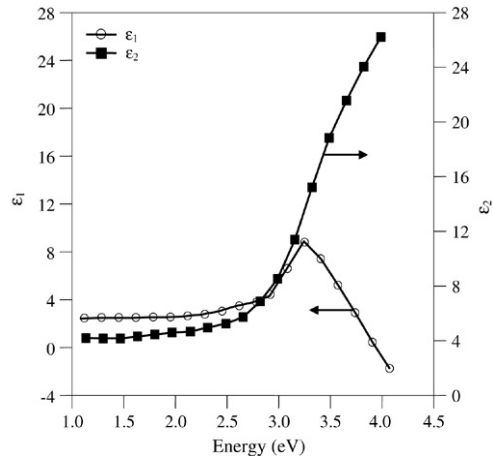


Fig. 5. Real ( $\epsilon_1$ ) and imaginary ( $\epsilon_2$ ) parts of the dielectric function as a function of photon energy for the ZnO thin film.

compound has a significant effect on the optical properties of the thin film.

The refractive index  $n(\lambda)$  was evaluated from the optical transmittance spectra using the well-known Swanepoel's envelope method as described in Eq. (3). For this purpose upper and lower envelopes were drawn to the transmittance curves in Fig. 2. And also K–K relations were used to calculate refractive index as a function of wavelength. The variations of refractive index  $n$  with wavelength in the region 400–700 nm are shown in Fig. 4 and the results were consistent for both techniques. The value of refractive index  $n$  is decreased with increasing wavelength as shown in Fig. 4. The increase in the refractive index is associated with fundamental band gap absorption.

### 3.3. Determination of complex dielectric functions and oscillator energy

We have used reflectance spectra of zinc oxide thin film in the ultraviolet range. The real and imaginary parts of the dielectric coefficient have been calculated using Eq. (8) and are plotted as a function of photon energy in Fig. 5. The energy band gap is determined from the spectra of the real dielectric

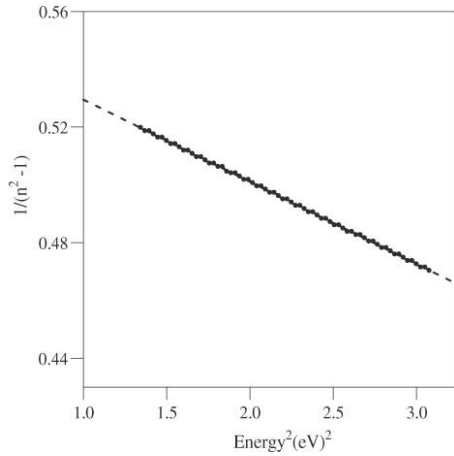


Fig. 6. Experimental values and single electronic oscillator model fit curve as a function of  $(1/\lambda^2)$  for the ZnO thin film deposited on glass substrate.

coefficient and the value is 3.24 eV which is in agreement with the experimental value.

Fig. 6 shows the relation between  $(n^2 - 1)^{-1}$  and  $E^2$  for the ZnO thin film. The values of  $E_{osc}$  and  $E_d$  are directly determined from the slope,  $(E_{osc}E_d)^{-1}$ , and the intercept,  $(E_{osc}/E_d)$ . The equation for the best fitting straight line was used to calculate dispersion and oscillator energy. The equation for the best fitting straight line was found to be:

$$\frac{1}{(n^2(E) - 1)} = -0.028 \times E^2 + 0.557$$

where  $E$  is the energy of the photon in eV. Dispersion and oscillator energy was found to be  $E_d = 8$  eV,  $E_{osc} = 4.46$  eV respectively.

The long wavelength refractive index ( $n_\infty$ ), average oscillator wavelength ( $\lambda_0$ ) and oscillator length strength  $S_0$  parameters for the ZnO thin film can be determined by the single oscillator model given by [33]

$$\frac{(n_\infty^2 - 1)}{(n^2 - 1)} = 1 - \left(\frac{\lambda_0}{\lambda}\right)^2 \tag{12}$$

The  $n_\infty$  value for the ZnO thin film was obtained from the linear parts of  $(n^2 - 1)^{-1}$  vs  $\lambda^{-2}$  curves.

Rearranging of Eq. (12) gives

$$n^2 - 1 = \frac{S_0^2 \lambda_0^2}{(1 - \lambda_0^2/\lambda^2)} \tag{13}$$

where  $S_0 = \frac{(n_\infty^2 - 1)}{\lambda_0^2}$  is the average oscillator parameter which is the strength of the individual dipole oscillator. The  $S_0$  value for the ZnO thin film was calculated using Eqs. (12) and (13). The equation for the best fitting straight line was found to be:

$$\frac{1}{(n^2(\lambda) - 1)} = -43.732x \frac{1}{\lambda^2} + 0.5579$$

where  $\lambda$  is in nm. Oscillator length strength and  $n_\infty$  for the ZnO thin film were found to be  $2.2 \times 10^{-5} \text{ nm}^{-2}$  and 1.67, respectively. The value of static dielectric constant,  $\epsilon_\infty = n^2(0)$ , was also calculated and found to be 2.78.

Table 1  
The comparison results of this study with the published data

References	Thickness (nm)	Band gap (eV)	Refractive index	Grain size (nm)
In this study	357	3.22–3.24	(at 500 nm) 1.832	22.5
[35]	300–350	(at 500 nm) 3.24–3.32	(at 500 nm) 1.94–2.03	25–55
[36]	300	3.25–3.275	(at 632.8 nm) 1.97–1.93	26–32
[37]	200–600	3.27–3.30		18.98–19.88

Dispersion energy  $E_d$  obeys a simple empirical relationship as  $E_d = \beta N_c Z_a N_e$  eV. In this equation,  $N_c$  is the coordination number of the nearest-neighbor cation,  $Z_a$  the formal anion valence, and  $N_e$  the effective number of valence electrons per anion.  $\beta$  is constant and has the value of 0.123 eV using the published data for  $N_c$ ,  $Z_a$  and  $N_e$  [34].

Table 1 shows some results of 357 nm as-deposited ZnO thin film by comparing with the published data; we conclude that pulsed filtered cathodic vacuum arc deposition is a suitable film deposition technique to obtain very similar properties.

#### 4. Conclusion

In conclusion, the optical and structural properties of the PFCVAD ZnO thin film on glass substrate have been investigated by transmittance, absorption and reflection measurements in the wavelength range of 190–1100 nm. The refractive index  $n$ , the absorption coefficient  $\alpha$  and the film thickness  $t$  were determined from transmission and reflection data. Kramers–Kronig analysis of reflectance spectra has successfully been used to determine the refractive index and extinction coefficient of the ZnO thin film as a function of the wavelength. These results were consistent with the results that were obtained from the envelope method. The differences between the values obtained with these methods were found to be higher at the near optical band edge region (480–490 nm) and at the long wavelength region. The complex dielectric function was calculated using Kramers–Kronig relations. The dispersion of the refractive index in the transparent region is interpreted successfully in terms of a single electronic oscillator model.

The structural and optical quality of ZnO thin films deposited using PFCVAD at 25 °C is consistent with that of ZnO thin films deposited using other growth techniques, indicating that the PFCVAD method is very effective in facilitating film growth at room temperature. All these results suggest that PFCVAD is a useful technique to produce high quality polycrystalline ZnO thin films at low temperature for device applications such as TFT, UV detector, p–n diodes etc.

#### Acknowledgment

This work was supported by the Research Fund of the University of Cukurova, Adana, Turkey (Project No: 2004K120360-7).

**References**

- [1] A.L. Dower, J.C. Joshi, *Mater. Sci.* 19 (1984) 1.
- [2] J.A. Ronovich, D. Golmoya, R.H. Bube, *J. Appl. Phys.* 51 (1980) 4260.
- [3] K.L. Chopra, S. Major, D.K. Pandya, *Thin Solid Films* 102 (1983) 1.
- [4] A. Malik, A. Seco, P. Nunes, M. Vieira, E. Fortunato, R. Martins, Flat panel display materials III, in: *MRS Proc.*, vol. 471, Materials Research Society, p. 47.
- [5] E. Shanti, A. Banerjee, K.L. Chopra, *Thin Solid Films* 108 (1983) 333.
- [6] T.L. Tansley, D.F. Neely, C.P. Foley, *Thin Solid Films* 117 (1984) 19.
- [7] P. Nunes et al., *Vacuum* 52 (1999) 45.
- [8] J. Hu, R.G. Gordon, *J. Appl. Phys.* 71 (1992) 880.
- [9] S. Oda, H. Tokunaga, N. Kitajama, J. Hanna, I. Shimizu, H. Kokado, *Japan. J. Appl. Phys.* 24 (1985) 1607.
- [10] T. Minami, K. Oohashi, S. Takata, T. Mouri, N. Ogawa, *Thin Solid Films* 193/194 (1990) 721.
- [11] T. Minami, H. Sato, H. Nanto, S. Takata, *Japan. J. Appl. Phys.* 24 (1985) L781.
- [12] Y. Igasaki, H. Saito, *J. Appl. Phys.* 70 (1991) 3613.
- [13] A.F. Aktaruzzaman, G.L. Sharma, L.K. Malhotra, *Thin Solid Films* 198 (1991) 67.
- [14] D. Goyal, P. Solanki, B. Marathe, M. Takwale, V. Bhide, *Japan. J. Appl. Phys.* 31 (1992) 361.
- [15] A. Suzuki, T. Matsushita, N. Wada, Y. Sakamoto, M. Okuda, *Japan. J. Appl. Phys.* 35 (1996) L56.
- [16] H. Hiramatsu, K. Imaeda, H. Horio, M. Nawata, *J. Vac. Sci. Technol. A* 16 (1998) 669.
- [17] M. Naoue, S. Nakagawa, *IEEE Trans. Magn.* 29 (1993) 3096.
- [18] H. Takikawa, K. Kimura, R. Miyano, T. Sakakibara, *Thin Solid Films* 377–378 (2000) 74.
- [19] P.A. Lindfors, W.M. Mularie, *Surf. Coat. Technol.* 29 (1986) 275.
- [20] E. Şenadım, H. Kavak, R. Esen, *J. Phys.: Condens. Matter* 18 (2006) 6391.
- [21] D. Minkov, R. Swanepoel, *Opt. Eng.* 32 (1993) 3333.
- [22] Y. Laaziz, A. Bennouna, *Thin Solid Films* 277 (1996) 155.
- [23] J.M. Gonzalez-Leal, E. Marquez, A.M. Bernal-Oliva, J.J. Ruiz-Perez, R. Jimenez-Garay, *Thin Solid Films* 317 (1998) 223.
- [24] R. Rusli, G.A.J. Amaratunga, *Appl. Opt.* 34 (1995) 7914.
- [25] V. Pandey, N. Mehta, S.K. Tripathi, A. Kumar, *Chal. Lett.* 2/5 (2005) 39.
- [26] M.G. Sceats, G.C. Morris, *Phys. Status Solidi A* 14 (1972) 643.
- [27] F.W. King, *J. Chem. Phys.* 71 (11) (1979) 4726.
- [28] B. Harbecke, *Appl. Phys. A* 40 (1986) 151.
- [29] J.E. Bertie, S.L. Zhang, *Can. J. Chem.* 70 (1992) 520.
- [30] S.H. Wemple, M. DiDomenico, *Phys. Rev. Lett.* 23 (1969) 1156.
- [31] J. Tauc, R. Grigorvici, A. Vancu, *Phys. Status Solidi* 15 (1966) 627.
- [32] F. Urbach, *Phys. Rev.* 92 (1953) 1324.
- [33] F. Yakuphanoglu, M. Durmuş, M. Okutan, O. Köysal, V. Ahsen, *Physica B* 373 (2006) 262.
- [34] S.H. Wemple, M. DiDomenico, *Phys. Rev. B* 3 (1971) 1338.
- [35] T.K. Subramanyam, B. Srinivasulu Naidu, S. Uthanna, *Cryst. Res. Technol.* 35 (2000) 1193.
- [36] A. Moustaghfir, E. Tomasellaa, S. Ben Amor, M. Jacquet, J. Cellier, T. Sauvage, *Surf. Coat. Technol.* 174/175 (2003) 193.
- [37] S.S. Lin, J.L. Huang, *Surf. Coat. Technol.* 185 (2004) 222.